

# Coherent control of cavity quantum electrodynamics for quantum nondemolition measurements and ultrafast cooling

Ren-Bao Liu, Wang Yao, and L. J. Sham

*Department of Physics, University of California San Diego, La Jolla, California 92093-0319*

(Received 22 June 2005; published 17 August 2005)

Quantum nondemolition measurements and ultrafast cooling of single spins are critical for scalable quantum computation. For such purposes, quantum evolution in a coupled structure of a nanodot, a microcavity, and a waveguide can be coherently controlled to establish efficient quantum pathways connecting in sequence an electron spin, a charged exciton, a cavity photon, and finally a flying photon in the waveguide. As an example of suppressing unwanted dynamics in complex solid-state systems, pulse shaping is employed to switch the nanodot-cavity coupling on demand and to perform robust quantum operation.

DOI: [10.1103/PhysRevB.72.081306](https://doi.org/10.1103/PhysRevB.72.081306)

PACS number(s): 78.67.Hc, 03.67.Lx, 42.50.Pq, 78.47.+p

Cooling or initialization in ultrafast time scales is a prerequisite for coherent optical control of single spins, especially for quantum computation, which requires a continuous reset of qubits for quantum error correction.<sup>1</sup> On the other hand, the quantum measurement of single electron spins is notoriously difficult. The existing schemes of single-spin measurement<sup>2-6</sup> are mostly based on electrical measurement via spin-charge conversion and thus is incompatible with ultrafast optical control of spins.

Quantum nondemolition (QND) measurement is critical for scalable quantum computation. In quantum computation, the final state before measurement is in general a superposition of the basis states, written as  $\sum C_x |x\rangle$ , and a measurement in the basis gives an output  $x$  from which the result is derived. In practice, to establish statistical confidence or accumulate signal strength by imperfect detection, the measurement should be repeated to have a certain  $x$  observed at least twice. In a destructive measurement, each cycle has to be started with a fresh preparation of the final state and could result in any possible output  $x$ , which amounts to measuring an ensemble of identical quantum states (similar to identical molecules used in NMR-based quantum computation). When the number of qubits (problem size) increases, the number of basis states  $|x\rangle$  in the superposition could increase exponentially, as in the famous Shor algorithm for factorization<sup>7</sup>; thus, the physical resources, being the number of repeated cycles or the ensemble size, would scale up exponentially. By contrast, in a QND measurement, a state collapses into a basis state and remains in it for the repeated cycles; thus the signal strength can be accumulated with a limited number of repetitions, similar to the cycling transitions used for single ions.<sup>8-10</sup>

In this paper, we illustrate the idea of using single-shot coherent quantum evolution to realize ultrafast cooling and QND measurement of single electron spins, in the coupled system of a doped quantum dot, a microcavity, and a waveguide. The directed one-dimensional photon continuum and coherent optical control of the cavity quantum electrodynamics (QED) provide the means of manipulating irreversible photon-emission processes. The cooling and measurement, as unitary quantum transformations, conserve the entropy or quantum information, which is essential for quantum error

diagnosis and quantum feedback control. Cooling and measurement via single-shot quantum evolution should be the ultimate paradigm of controlling the interaction between macroscopic environments (or instruments) and microscopic quantum systems, which is central to nanosciences, especially in molecular electronics and quantum computation. The unitary transformation, including the controllable environment (photons in the waveguide), is significantly different from the quantum jumps proposed for spin-qubit readout.<sup>11,12</sup>

The present paper is based on a series of theoretical and experimental advances in optical microstructures<sup>13-16</sup> and in cavity QED of single quantum dots,<sup>17-22</sup> particularly including the very recent demonstration of the strong coupling between single quantum dots and microcavities.<sup>21,22</sup> Our present paper outlines a direction for current research on cavity QED of single solid-state systems such as quantum dots and impurities, as the studies of the cavity QED of single atoms have led to fundamental knowledge of atom dynamics and to applications in quantum information science,<sup>23-26</sup> particularly including the state transfer between atoms and photons.<sup>25,26</sup> Since cavity-assisted reversible quantum operations on spin qubits in quantum dots have been proposed,<sup>27</sup> here we concentrate on the control of irreversible QED process, with notable examples of ultrafast cooling and the QND measurement of single spins.

Error sources that cause the most concern in solid-state quantum computation, specifically in optically controlled quantum-dot systems, are irreversible photon emission during qubit operations, nonresonant excitation of unwanted levels, imperfect selection rules, and system parameter uncertainty. The idea of suppressing such errors by shaping the controlling laser pulse will be demonstrated in this paper through two examples: The on-demand switch of dot-cavity coupling by the ac Stark effect can avoid spontaneous emission during qubit operations, and chirped pulses can perform Rabi flops robust against parameter uncertainty.

The basic idea of controlling cavity QED is depicted in Fig. 1. A high-quality cavity attached to a nanodot modifies the electromagnetic vacuum in the vicinity of the  $n$ -doped dot via the coupling between the evanescent wave of the whispering gallery modes in the cavity and the electronic transitions in the dot. A waveguide coupled to the cavity<sup>13</sup>

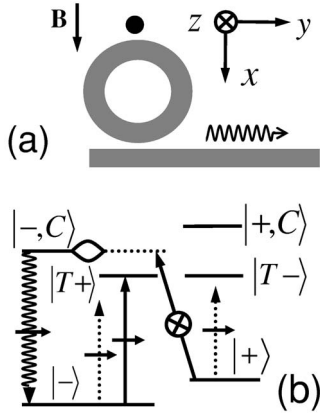


FIG. 1. (a) Schematics of the dot-cavity-waveguide coupling structure. (b) Basic optical processes for cooling and measuring a spin state. The dotted, solid, and wavy arrows represent the ac Stark pulse, the tipping pulse, and the spontaneous emission, respectively. X and Y polarizations are indicated by the horizontal arrows and circled cross, respectively.

acts as a quantum channel into which the cavity photon can escape rapidly to a designated destination such as a detector. The qubit is represented by the electron spin states  $|\pm\rangle \equiv e_{\pm}^{\dagger}|G\rangle$  ( $|G\rangle$  is the crystal ground state), split by a static magnetic field in the  $x$  direction. Optical excitations lead to two degenerate trion states  $|T\mp\rangle \equiv (h_{3/2}^{\dagger} \pm h_{-3/2}^{\dagger})e_{\pm}^{\dagger}|G\rangle$  ( $h_{\pm 3/2}^{\dagger}$  creates a heavy hole with angular momentum  $\pm 3/2$  along the growth direction). Thus an X- or Y-polarized tipping pulse will flip  $|\pm\rangle$  to  $|T\mp\rangle$  or  $|T\pm\rangle$ , respectively.<sup>28</sup> The trion states are, by design, off resonant from the cavity modes to avoid cavity-induced optical decoherence during quantum operations of the spin. When the nanodot-cavity coupling is desired, the trion transitions and the cavity mode  $|C\rangle$  may be driven by a laser pulse into resonance via the ac Stark effect. The evanescent wave of the cavity mode is designed to be X polarized in the vicinity of the nanodot, so that when brought within resonance, the trion states  $|T\pm\rangle$  and the cavity states  $|\mp, C\rangle$  are coupled into two split trion-polariton states, respectively. This provides a fast decay of the trion to a spin state by emitting a photon into the quantum channel. A choice of the polarization of the tipping pulse can either (1) use the quantum channel as an entropy dump for the process of cooling the spin to the ground state, or (2) entangle the spin qubit with a photon qubit in the quantum channel, thus enabling the QND measurement of the spin qubit via photon detection.

The detailed optical processes of cooling a spin qubit are illustrated in Fig. 2(a). While the system must be maintained at a sufficiently low temperature for the preservation of spin coherence, it does no harm to assume that the doped electron is initially in an unpolarized state, i.e.,  $\hat{\rho}(-\infty) = 0.5|-\rangle\langle -| + 0.5|+\rangle\langle +|$ . A cooling cycle consists of four basic steps: (1) An X-polarized ac Stark pulse is adiabatically switched on, bringing the states  $|T+\rangle$  and  $|- , C\rangle$  into resonance. (2) A Y-polarized tipping pulse flips the spin up state  $|+\rangle$  to the polariton states formed by  $|T+\rangle$  and  $|- , C\rangle$ . (3) The polariton states relax to the spin-down state  $|-\rangle$  rapidly by emitting a photon into the waveguide, dumping the spin entropy to the

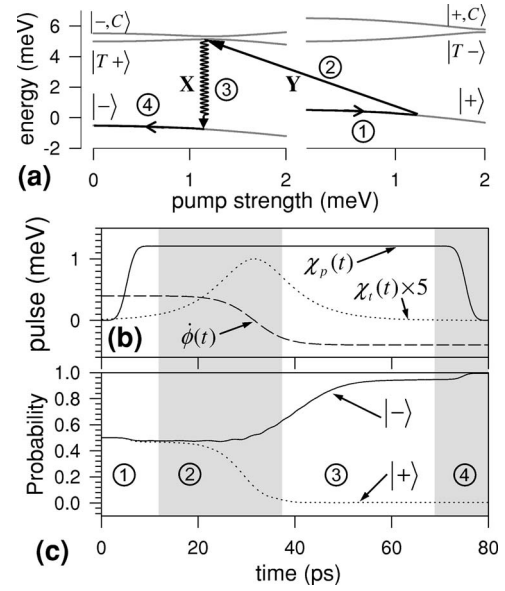


FIG. 2. (a) Detailed optical process for spin initialization. The gray curves are the energies of different states vs the Rabi frequency of the ac Stark pulse, in the rotating frame. (b) The Rabi frequencies of the ac Stark pulse and the tipping pulse (amplified by a factor 5), and the sweeping frequency of the tipping pulse. (c) Probabilities of spin down and up. Different steps of the cooling cycle, indicated by ①–④, are distinguished by shadowed areas in (b) and (c).

environment. (4) The ac Stark pulse is adiabatically switched off. No photon generation or spin flip would take place if the initial spin state were  $|-\rangle$ . Thus ideally, after the cooling cycle, the spin is fully polarized with the entropy mapped into the quantum channel, and the final density matrix becomes  $|-\rangle\langle -| \otimes (0.5|0\rangle\langle 0| + 0.5|1\rangle\langle 1|)$ , where  $|n\rangle$  is the  $n$ -photon waveguide state.

The cooling process has been simulated by numerically solving the master equation of the dot-cavity system

$$\partial_t \hat{\rho} = -i[\hat{H}, \hat{\rho}] - \frac{\gamma + \gamma'}{2} \mathcal{L}_{\hat{a}} \hat{\rho} - \frac{\Gamma}{2} \sum_{s,s'=\pm} \mathcal{L}_{|s\rangle\langle Ts'|} \hat{\rho}, \quad (1)$$

$$\begin{aligned} \hat{H} \equiv & \Omega_C \hat{a}^{\dagger} \hat{a} \pm \frac{\omega_L}{2} |\pm\rangle\langle \pm| + \Omega_T |T\pm\rangle\langle T\pm| + g_{\text{cav}} |T\pm\rangle\langle \mp| \hat{a} \\ & + \text{H.c.} + [\chi_t(t) \mathbf{e}_t + \chi_p(t) \mathbf{e}_p] \cdot \mathbf{e}_X (|T\pm\rangle\langle \mp| + r_C \hat{a}^{\dagger}) + \text{H.c.} \\ & + [\chi_t(t) \mathbf{e}_t + \chi_p(t) \mathbf{e}_p] \cdot \mathbf{e}_Y |T\pm\rangle\langle \pm| + \text{H.c.}, \end{aligned} \quad (2)$$

$$\mathcal{L}_{\hat{a}} \hat{\rho} \equiv 2\hat{a} \hat{\rho} \hat{a}^{\dagger} - \hat{a}^{\dagger} \hat{a} \hat{\rho} - \hat{\rho} \hat{a}^{\dagger} \hat{a}, \quad (3)$$

where  $\gamma$  is the cavity-waveguide escape rate,  $\gamma'$  is the cavity-free-space loss rate,  $\Gamma$  is the trion decay rate due to spontaneous emission into free space,  $\hat{a}$  annihilates a cavity photon,  $r_C$  is the ratio of pump strength of the cavity mode to that of the trions by control pulses, the subscripts  $t$  and  $p$  denote the tipping and ac Stark pulses, respectively, and the other notations are self-explanatory. Realistic parameters have been chosen as follows: The Zeeman splitting  $\omega_L = 1$  meV,  $\gamma = 0.2$  meV,  $\gamma' = 0.045$   $\mu\text{eV}$  (corresponding to an intrinsic Q

factor  $\sim 3 \times 10^7$ ), the dot-cavity coupling  $g_{\text{cav}}=0.1$  meV, the cavity-trion detuning  $\Omega_C - \Omega_T - \omega_L/2 = 0.5$  meV,  $\Gamma = 1$   $\mu\text{eV}$ , and  $r_C = 0.3$ .

The control of the nanodot-vacuum coupling is provided by shaping the pump and tipping pulses. The ac Stark pulse has an almost-square profile as

$$\chi_p(t) = \chi_p e^{-i\Omega_p t} \{\text{erf}[\sigma_p(t-t_1)] - \text{erf}[\sigma_p(t-t_2)]\},$$

[see Fig. 2(b)] and is  $X$  polarized ( $\mathbf{e}_p = \mathbf{e}_X$ ). The spectral width ( $\sigma_p = 0.354$  meV) is set much smaller than the detuning ( $\Omega_T + \omega_L/2 - \Omega_p = 5.5$  meV), so that the effect due to nonadiabatic switch on and off is negligible. For the parameters given above, the trion state  $|T+\rangle$  and the cavity state  $|-,C\rangle$  are brought into resonance when the pump strength ( $2\chi_p$ ) reaches the value 1.21 meV. As the pump pulse maintains the resonant cavity-dot tunneling, which facilitates the photon escape to the quantum channel, the trion state relaxes very fast (on the time scale of  $g_{\text{cav}}^{-1}$  and  $\gamma^{-1}$ ,  $\sim 10$  ps). A duration of the pump pulse  $t_2 - t_1 = 70$  ps is found sufficient for the total dissipation of the photon. The tipping pulse ideally should be a  $\pi$  pulse for Rabi oscillation between  $|+\rangle$  and  $|T+\rangle$ . Due to the dynamical nature of the states (dressed by the ac Stark pulse) and the rather small polariton splitting ( $\sim 0.1$  meV), a perfect  $\pi$  rotation requires an extremely long pulse. The solution is to shape a chirped pulse as  $\chi_t(t) = \chi_t e^{-i\phi(t) - i\Omega_t t} \text{sech}[\sigma_t(t-t_t)]$  with the phase sweeping rate  $\dot{\phi}(t) = -\sigma_c \tanh[\sigma_t(t-t_t)]$ .<sup>29</sup> The frequency of the pulse now will sweep from  $\sigma_c$  above  $\Omega_t$  to  $\sigma_c$  below. When the sweeping range  $[\Omega_t - \sigma_c, \Omega_t + \sigma_c]$  covers both of the trion-polariton states, the initial spin state  $|+\rangle$  will be left adiabatically in a superposition of the two polariton states, which relaxes rapidly to the target spin state  $|-\rangle$ . In simulation, the tipping pulse, with frequency sweeping range  $\sigma_c = 0.4$  meV, strength  $\chi_t = 0.2$  meV, and duration  $1/\sigma_t = 6.58$  ps, flips the spin state  $|+\rangle$  to the polariton states with negligible error. Such a geometrical flip is insensitive to transition frequency and strength,<sup>29</sup> and thus can tolerate to some degree laser fluctuations and uncertainty in dipole moment, transition energy, and selection rules.

Figure 2(c) shows that a single cooling cycle completed within 80 ps produces an almost 100% polarized spin from a maximally mixed state. The multiphoton cavity states were included in the numerical calculation, as they renormalize the ac Stark shift (the real excitation of multiphoton states is negligible due to the off-resonance condition). Inclusion of up to three-photon states was found sufficient to obtain converged results. The density matrix at the end of the cycle is  $\hat{\rho} = 0.9945|-\rangle\langle -| + 0.0040|+\rangle\langle +| + \hat{\rho}_{\text{err}}$ , where  $\hat{\rho}_{\text{err}}$  is the probability ( $\approx 0.15\%$ ) of the system remaining in the trion states, which results mainly from the nonadiabatic switching of the ac Stark pulse. The decay of the trion and the cavity modes by emitting photons into free-space constitute the main error source ( $\approx 0.4\%$ ), as the trion state relaxes to different spin states depending on the polarization of the emitted free-space photon.

A mere switch of the polarizations of the tipping and pump pulses from  $(Y, X)$  to  $(X, Y)$ , respectively, changes the “cooling” operation to a “measurement” one. The measure-

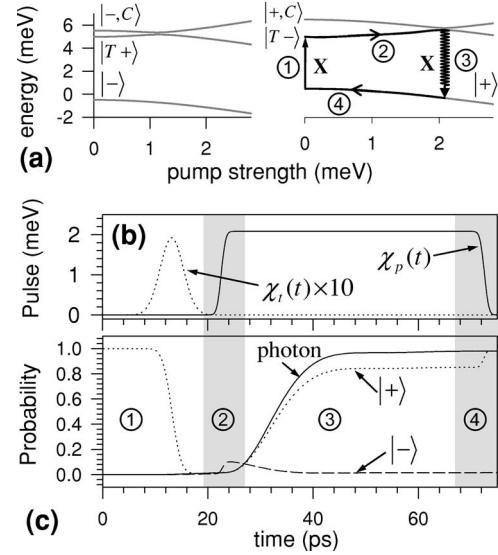


FIG. 3. (a) Detailed optical process for the measurement cycle. (b) The Rabi frequencies of the ac Stark pulse and the tipping pulse (amplified by a factor 10). (c) Probabilities of spin down and up, and the number of waveguide photons, for a spin initially polarized up.

ment cycle includes four basic steps [see Fig. 3(a)]: (1) An  $X$ -polarized tipping pulse flips the spin state  $|+\rangle$  to the trion state  $|T-\rangle$ . (2) A  $Y$ -polarized ac Stark pulse adiabatically switched on drives the trion state into resonance with the cavity state  $|+,C\rangle$ . (3) The trion state resonantly tunnels into the cavity state and relaxes rapidly back to the spin state  $|+\rangle$ , leaving a photon emitted into the quantum channel. (4) The ac Stark pulse is adiabatically switched off. Suppose that the spin state to be measured is  $\alpha|+\rangle + \beta|-\rangle$  and the channel is initially in the vacuum state  $|0\rangle$ . The measurement process will ideally transform the system into the entangled state  $\alpha|+\rangle|1\rangle + \beta|-\rangle|0\rangle$ , so that the detection of the photon projects the electron into a spin eigenstate, providing a QND measurement of the spin.

Note that the pulse timing for measurement is different from that for cooling [cf. Fig. 3(b) and Fig. 2(b)]. The measurement sequence has been designed to minimize the real excitation of the multiphoton states, while the cooling sequence has been designed to minimize the emission of free-space photons by the trion states. In measurement, the Rabi flop between the spin state and the trion is well separated in frequency from the cavity mode so that chirping the pulse is unnecessary. Instead, a simple Gaussian  $\pi$  pulse  $\chi_t(t) = \chi_t e^{-\sigma_t^2(t-t_t)^2/2 - i\Omega_t t}$  is used. The ac Stark pulse is chosen  $Y$  polarized to avoid direct excitation of the cavity mode.

The measurement cycle has been numerically simulated for the same structure as in Fig. 2. The number of photons emitted into the waveguide is calculated with  $\partial_t n = \gamma(\hat{a}^\dagger \hat{a})$ . The tipping and the AC Stark pulses are set such that  $1/\sigma_t = 2.19$  ps,  $\chi_t = 0.192$  meV,  $\Omega_t = \Omega_T - \omega_L/2$ ,  $\sigma_p = 0.707$  meV,  $2\chi_p = 2.08$  meV,  $\Omega_T + \omega_L/2 - \Omega_p = 5.5$  meV, and the duration of the pump pulse  $t_2 - t_1 = 50$  ps. After a single cycle of measurement with an initial state  $\hat{\rho}_0 = |+\rangle\langle +|$  results in the final state  $\hat{\rho}_1 = 0.0161|-\rangle\langle -| + 0.9824|+\rangle\langle +| + \hat{\rho}_{\text{err}}$  with the number of

photon emitted into the waveguide  $n=0.9806$  [see Fig. 3(c)], while an initial state  $\hat{\rho}_0=|-\rangle\langle-|$  results in the final state  $\hat{\rho}_1=0.9955|-\rangle\langle-|+0.0040|+\rangle\langle+|+\hat{\rho}_{\text{err}}$  with  $n=0.0015$  (not shown). The photon emitted into the waveguide can be detected with high efficiency.<sup>30</sup> If the detector has zero dark-count rate and efficiency of 50%, the POVM (positive operator-valued measures) for the measurement process can be defined as  $\hat{P}_-\equiv 0.9992|-\rangle\langle-|+0.5097|+\rangle\langle+|$  and  $\hat{P}_+\equiv 0.0008|-\rangle\langle-|+0.4903|+\rangle\langle+|$ . Within five measurement cycles, the spin state can be measured with accuracy higher than 97%, and the back-action noise to the spin is less than 10%, while the time duration is less than 0.4 ns, much shorter than the spin decoherence time.

In summary, the coupling between the electromagnetic fields and the nanodot can be customized both by spatially assembling microresonators and quantum channels in the vicinity of the dot and by temporal design of the control optical pulses. Such a control can speed up the spontaneous decay of the excited state in the dot leading to ultrafast cooling and QND measurement of a single electron spin. The specific

micro-ring-waveguide structure may be replaced by equivalent waveguide-resonator systems such as microsphere-fiber structures<sup>13</sup> and line- and point-defects engineered in photonic crystals.<sup>16,17</sup> In the numerical simulations, we attempted to take care of the primary sources of errors, including the optical decoherence, unintended dynamics involving states not desired, either by stating their estimated size if not negligible or by designing the processes to limit their effect. The strong electron-cavity photon coupling assumed in the numerical simulations of the initialization and measurement operations turns to be reasonable by the new findings.<sup>21,22</sup> Moreover, efficiency reduction as a consequence of lower  $Q$  values can be tolerated by recycling the operations a few times. The schemes proposed here may also be adapted to monitor and control the spin state of a single molecule<sup>31</sup> adsorbed on a cavity-waveguide structure.

This work was supported by ARDA/ARO Contract No. DAAD19-02-1-0183, NSF Grant No. DMR-0099572, and QuIST/AFOSR Contract No. F49620-01-1-0497.

- 
- <sup>1</sup>D. DiVincenzo, *Fortschr. Phys.* **48**, 771 (2000).  
<sup>2</sup>M. Xiao, I. Martin, E. Yablonovitch, and H. W. Jiang, *Nature (London)* **430**, 435 (2004).  
<sup>3</sup>H.-A. Engel *et al.*, *Phys. Rev. Lett.* **93**, 106804 (2004).  
<sup>4</sup>R. Ionicioiu and A. E. Popescu, *New J. Phys.* **7**, 120 (2005).  
<sup>5</sup>J. M. Elzerman *et al.*, *Nature (London)* **430**, 431 (2004).  
<sup>6</sup>M. Friesen, C. Tahan, R. Joynt, and M. A. Eriksson, *Phys. Rev. Lett.* **92**, 037901 (2004).  
<sup>7</sup>P. W. Shor, *SIAM J. Comput.* **26**, 1484 (1997).  
<sup>8</sup>C. A. Sackett *et al.*, *Nature (London)* **404**, 256 (2000).  
<sup>9</sup>A. Imamoglu, *Phys. Rev. Lett.* **89**, 163602 (2002).  
<sup>10</sup>D. F. V. James and P. G. Kwiat, *Phys. Rev. Lett.* **89**, 183601 (2002).  
<sup>11</sup>A. Imamoglu, *Fortschr. Phys.* **48**, 987 (2000).  
<sup>12</sup>T. Calarco, A. Datta, P. Fedichev, E. Pazy, and P. Zoller, *Phys. Rev. A* **68**, 012310 (2003).  
<sup>13</sup>S. M. Spillane, T. J. Kippenberg, O. J. Painter, and K. J. Vahala, *Phys. Rev. Lett.* **91**, 043902 (2003).  
<sup>14</sup>D. K. Armani, T. J. Kippenberg, S. M. Spillane, and K. J. Vahala, *Nature (London)* **421**, 925 (2003).  
<sup>15</sup>S. C. Hagness, S. T. Ho, and A. Taflove, *J. Lightwave Technol.* **15**, 2154 (1997).  
<sup>16</sup>Y. Akahane, T. Asano, B.-S. Song, and S. Noda, *Nature (London)* **425**, 944 (2003).  
<sup>17</sup>S. Hughes and H. Kamada, *Phys. Rev. B* **70**, 195313 (2004).  
<sup>18</sup>X. D. Fan, P. Palinginis, S. Lacey, H. L. Wang, and M. C. Lonergan, *Opt. Lett.* **25**, 1600 (2000).  
<sup>19</sup>M. Pelton *et al.*, *Phys. Rev. Lett.* **89**, 233602 (2002).  
<sup>20</sup>A. Kiraz *et al.*, *J. Opt. B: Quantum Semiclassical Opt.* **5**, 129 (2003).  
<sup>21</sup>J. P. Reithmaier *et al.*, *Nature (London)* **432**, 197 (2004).  
<sup>22</sup>T. Yoshie *et al.*, *Nature (London)* **432**, 200 (2004).  
<sup>23</sup>H. Mabuchi, J. Ye, and H. J. Kimble, *Appl. Phys. B: Lasers Opt.* **68**, 1095 (1999).  
<sup>24</sup>S. Haroche, *Philos. Trans. R. Soc. London, Ser. A* **361**, 1339 (2003).  
<sup>25</sup>J. I. Cirac, P. Zoller, H. J. Kimble, and H. Mabuchi, *Phys. Rev. Lett.* **78**, 3221 (1997).  
<sup>26</sup>L.-M. Duan, A. Kuzmich, and H. J. Kimble, *Phys. Rev. A* **67**, 032305 (2003).  
<sup>27</sup>A. Imamoglu *et al.*, *Phys. Rev. Lett.* **83**, 4204 (1999).  
<sup>28</sup>W. Yao, R. Liu, and L. J. Sham, *Phys. Rev. Lett.* **92**, 217402 (2004).  
<sup>29</sup>D. Goswami, *Phys. Rep.* **374**, 385 (2003).  
<sup>30</sup>S. Takeuchi, J. Kim, Y. Yamamoto, and H. H. Hogue, *Appl. Phys. Lett.* **74**, 1063 (1999).  
<sup>31</sup>J. Wrachtrup, C. von Borczyskowski, J. Bernard, M. Orrit, and R. Brown, *Nature (London)* **363**, 244 (1993).